Weierstraß–Institut
für Angewandte Analysis und Stochastik

im Forschungsverbund Berlin e.V.

Technical Report ISSN 1618 – 7776

Sampling techniques applicable for the characterization of the quality of self pulsations in semiconductor lasers

Mindaugas Radziunas[1,2]

submitted: 13th February 2002

[1] Weierstrass Institute for
Applied Analysis and Stochastics,
Mohrenstrasse 39
10117 Berlin
E-Mail: radziuna@wias-berlin.de

[2] Institute of Physics,
Humboldt University Berlin,
Invalidenstrasse 110
10115 Berlin

Technical Report No. 2
Berlin 2002

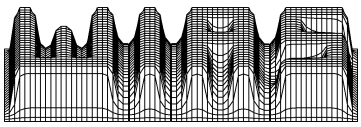

2000 *Mathematics Subject Classification.* 78-04,78-01,78A55.

Key words and phrases. Self pulsations, quality, locking, jitter.

This report is done within a BMBF project "Hochfrequente Selbstpulsationen in Mehrsektions-Halbleiterlasern: Analysis, Simulation und Optimierung", FKZ: 13N7978.

Edited by
Weierstraß–Institut für Angewandte Analysis und Stochastik (WIAS)
Mohrenstraße 39
D — 10117 Berlin
Germany

Fax: + 49 30 2044975
E-Mail (X.400): c=de;a=d400-gw;p=WIAS-BERLIN;s=preprint
E-Mail (Internet): preprint@wias-berlin.de
World Wide Web: http://www.wias-berlin.de/

Abstract

The aim of the presented report is to demonstrate how the sampling techniques can be used to characterize the quality of self pulsations in a multisection semiconductor laser and the synchronization of self pulsations with an optical or electrical periodically modulated signal. The developed tools are described and some examples are given.

1 Introduction

It was demonstrated theoretically as well as experimentally that three section semiconductor lasers with two distributed feedback (DFB) sections and an integrated phase tuning section in between can exhibit high frequency self pulsations (SP).

Let us consider first a laser with only one highly pumped DFB section. Here, another DFB section is pumped low just to keep carriers at transparency and serves as a dispersive reflector. Such a laser is able to demonstrate SP at 5-20 GHz frequency. These SP were attributed to dispersive self Q-switching (DQS) type [1, 2]. SP of that type occur mainly due to an instability of the maximum gain mode. Recent investigations have also shown an important influence of the supporting neighbouring mode [3]. It is worth to mention that a similar laser can also exhibit self pulsations of Petermann-Tager type at 20-40 GHz frequency [4]. The frequency of such SP is determined by the distance between neighbouring cavity modes.

Recently, even higher frequency SP were demonstrated in a laser with both highly pumped DFB sections [5]. Each of these DFB sections supports its own mode, and the mode spacing determines the frequency of SP. At the same time, these modes are common modes of the entire compound cavity, therefore they can be mutually coupled and are able to produce a stable SP. The modeling has shown the existence of well modulated SP with extremely high frequency (up to 1 THz). Experimentally, SP with 80 GHz frequency have been also demonstrated. It seems that only the speed limitation of the laboratory equipment have not allowed to measure higher frequencies.

For applications it is necessary that a high frequency SP can be synchronized with an external modulated signal. As it can be seen in experiments, not every self pulsating laser performs a good locking. Therefore, a proper modeling is required to understand the mechanisms of locking of high frequency SP to modulated external signals.

In the present report we consider a traveling wave (TW) model, which is based on a hyperbolic system of partial differential equations for the counter-propagating optical fields, the polarization equations approximating gain dispersion with a Lorentzian function and the carrier rate equations [6].

To solve and to investigate the model equations the software tool LDSL (Longitudinal Dynamics in Semiconductor Laser) is used. This software was developed to simulate and to analyse nonlinear longitudinal dynamics of the optical fields and carriers in multi-section semiconductor lasers. LDSL-tool is suited to investigate and to design lasers which exhibit various nonlinear effects such as self pulsations, hysteresis, mode switching [2, 5, 6], excitability [7], chaos, synchronisation of self pulsations to an external signal frequency [5]. More information about this software soon will be available in [8].

The main aim of this report is to demonstrate how the developed software allows to compute and to analyze the quality of SP. We will discuss the arising problems when identifying a precise frequency and a jitter of the SP in a free running laser. Another problem is an identification of the exact conditions where the SP lock to an external signal.

The paper is organized as follows: In the second section of this report we introduce the TW model and show different possibilities to modulate an injected current or an optical injection. In the third section we discuss possible criteria to characterize the quality of SP. Some different diagrams and measures for the jitter of SP are introduced. The fourth section is devoted to synchronization of SP. We discuss some laser parameters influencing the quality of SP. At the end of the report some conclusions are drawn.

2 Model of semiconductor DFB laser

2.1 Traveling wave model

The TW model is a system of partial differential equations describing the dynamics of the optical fields $\psi = (\psi^+, \psi^-)^T$, the polarization functions $p = (p^+, p^-)^T$ and the carrier densities $n = (n_1, \ldots, n_m)^T$ averaged over each section. $S_1, \ldots, S_m$ denote m different laser sections. The TW model is given by the following equations:

$$
\begin{aligned}
\frac{-i}{\nu}\frac{\partial}{\partial t}\psi^{\pm} &= \Big(\pm i\frac{\partial}{\partial z} - \delta + \frac{i\alpha}{2} - \frac{\alpha_H + i}{2}g(n)\Big)\psi^{\pm} - \kappa\psi^{\mp} + \frac{ig_P}{2}(\psi^{\pm} - p^{\pm}) + F_{sp}^{\pm};\\
-i\frac{d}{dt}p^{\pm} &= \omega_P p^{\pm} - i\gamma_P(\psi^{\pm} - p^{\pm}) \qquad \Rightarrow \qquad G(n,\omega) = g(n) - g_P\frac{(\omega_P - \omega)^2}{\gamma_P^2 + (\omega_P - \omega)^2};\\
\frac{d}{dt}n_k &= \frac{I_k(t)}{eV_k} - R_k(n_k) - \nu\Big[g_k(n_k)\frac{1}{l_k}\int_{S_k}\psi^*\psi dz - g_{P,k}\Re e\frac{1}{l_k}\int_{S_k}\psi^*(\psi - p)dz\Big];\\
\text{b.c.} \qquad & \psi^+(0,t) = r_0\psi^-(0,t) + a(t), \qquad \psi^-(L,t) = r_L\psi^+(L,t). \qquad (1)
\end{aligned}
$$

Here, in order to model a modulated electrical or optical injection we use time dependent functions $I(t)$ or $a(t)$, which enter the carrier rate equations for the corresponding section or the boundary conditions, respectively.

2.2 Modeling of modulated external signal

We represent the time dependent functions $I(t)$ and $a(t)$ describing modulation of the current or the external injected signal in the following manner:

$$I(t) = I_0 + b_1(t), \qquad a(t) = \sqrt{a_0 + a_1(t)}e^{i\eta t} \quad \Rightarrow \quad |a(t)|^2 = a_0 + a_1(t). \qquad (2)$$

In general, the functions $I(t)$ and $|a(t)|^2$ (which gives modulation of incoming signal power) can be described in the same way. We have introduced a few different possibilities to model electrical and optical modulated signals. These signals can be described by the following input parameters used in the program LDSL:

```
//*************************************************************************
// Parameters of current injection  modulation in the sections.
// These, corresponding to modtype=0 (no modulation) play no role. Other types:
// 1 - "sin" shaped modulation around mean injection value;
// 2 - "sin" shaped modulation from injection level;
// 3 - "step" shaped modulation around mean injection value;
// 4 - "step" shaped modulation from injection level;
// 5 - Gaussian shaped modulation around mean injection value;
// 6 - Gaussian shaped modulation from injection level;
// 7 - just short (two step) input at "modon" time moment;
// 8 - "trapesoidal" (lin. change, constant, lin. recover) variation of current.
se[se_Id;sc]       = [ 90,0.1,5.4]*1e-3; // injection current (A)
se[se_modtype;sc]  = [  0,  0,  0];      // type of current modulation
se[se_modon;sc]    = [0.2,  0,  0]*1e-9; // time of switching on (s)
se[se_modampl;sc]  = [ 45,  0,  0]*1e-3; // (+-) modulation amplitude (A)
se[se_modduty;sc]  = [0.2,  0,  0];      // dutycycle of modulation (periods)
se[se_modfreq;sc]  = [  2,  0,  0]*1e9;  // frequency of current modulation (Hz)
se[se_modrand;sc]  = [  0,  0,  0];      // random (1) or not (0) modulation
//*************************************************************************
// Parameters of forward input optical field  via facets.
// Types of modulation the same as for current modulation. Parameter "meanpow"
// here plays role of constant (background) current injection level.
re[re_iftype;rf]   = [  5, 0, 0, 0];     // type of injected frw. opt. signal
re[re_ifon;rf]     = [0.2, 0, 0, 0]*1e-9;// time, when modulation switched on(s)
re[re_ifmeanpow;rf]= [  2, 0, 0, 0]*1e-3;// mean (background) power of signal(W)
re[re_ifmodpow;rf] = [ -2, 0, 0, 0]*1e-3;// (+-) ampl. of  power modulation (W)
re[re_ifduty;rf]   = [0.2, 0, 0, 0];     // dutycycle of modulated power(period)
re[re_ifpfrq;rf]   = [ 10, 0, 0, 0]*1e9; // amplitude's modulation frequency(Hz)
re[re_ifofrq;rf]   = [ -8, 0, 0, 0]*1e-9;// wavelength (lam-lam0) of input (m)
re[re_ifrand;rf]   = [  1, 0, 0, 0];     // random(1) or not(0) signal
//*************************************************************************
time_modulation_on = 1; // start modulation at time given above(0) or time above
                        // + time moment, from which we continue computations(1)
//*************************************************************************
```

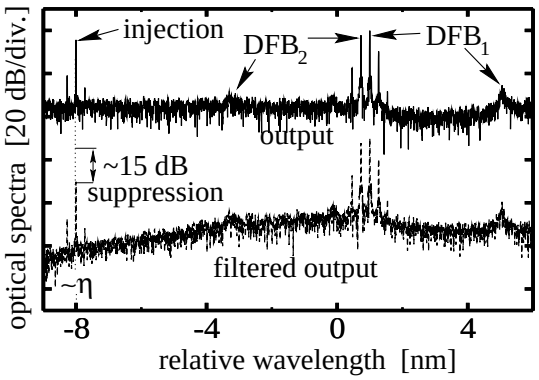

Figure 1: *Optical spectrum of the self pulsating (33 GHz) output in a 3 section laser with 2 active DFB sections. Upper and lower lines show spectra of the output without and with filtering respectively. The position of the resonances of each DFB section is indicated in the upper spectrum. The filter gives a 15 dB suppression at the wavelength of the injected optical signal.*

The meaning of these parameters is as follows:

- The parameter "re_ifofrq" is the relative wavelength of the injected optical signal and corresponds to the optical frequency η in (2). The wavelength of the injection can be seen in the optical spectrum of the output at Fig. 1.

- The parameters "se_modon" or "re_ifon" give the time moment t_0, when the modulation of the signal starts (see Fig. 2(a-e)).

  If, additionally, the parameter "time_modulation_on" $= 0$, then t_0 is an *absolute* time moment, counting from a first run of the program. This is very important when investigating the synchronisation of the fields, seeking to keep the modulation without any phase shift if continuing computations from the previous data.

  If the parameter "time_modulation_on" $= 1$, then t_0 is a *relative* time moment within the actually computed time interval.

- The parameters "se_modtype" and "re_iftype" describe different types of the modeled functions $b_1(t)$ and $a_1(t)$ respectively.

  Type *0*. There is no modulation at all, $I(t) = I_0$ and $a(t) = 0$.

  Types *1-6*. $b_1(t)$ and $a_1(t)$ are periodic functions describing a sequence of pulses. A profile of each single pulse is given by *sinusoidal* (types *1,2*), rectangular *step* (types *3,4*) or *Gaussian* (types *5,6*) functions (see Fig. 2(a-c)).

  Type *7*. A single short (two computational time steps) perturbation of the injected current or the optical signal (see Fig. 2(d)).

  Type *8*. A single "trapezoidal" variation of the current or the optical signal (see Fig. 2(e)).

- The parameters "se_Id" and "re_ifmeanpow" give either a background level of the pulses (types *2,4,6,7,8*), or the average of the functions $I(t)$ or $|a(t)|^2$ over a long time interval (types *1,3,5*).

- The parameters "se_modfreq" or "re_ifpfrq" represent the frequency f of the pulse trace (types *1-6*) or indicate the growth or the decay velocity of the single "trapezoidal" pulse (type *8*, see Fig. 2(e)).

- The parameters "se_modduty" or "re_ifduty" indicate a duty cycle d (full width at half maximum) of the single pulse (types *1-6*, Fig. 2(a-c)) or a width of the "trapezoidal" pulse at its maximal (minimal) value (type *8*, Fig. 2(e)). This value of d is given in the units of period $1/f$, i.e., the value of d/f is measured in seconds.

- The parameters "se_modampl" or "re_ifmodpow" give the amplitude A of the pulses (see Fig. 2(a-e)). Whenever negative values are adjusted to these amplitude parameters, holes or "negative" pulses are modeled (Fig. 2(c,e)).

- Finally, the parameters "se_modrand" and "re_ifrand" allow to model a sequence of the pulses (types *1-6*), which is generated by randomly selecting pulses from a periodic sequence (see Fig. 2(c)).

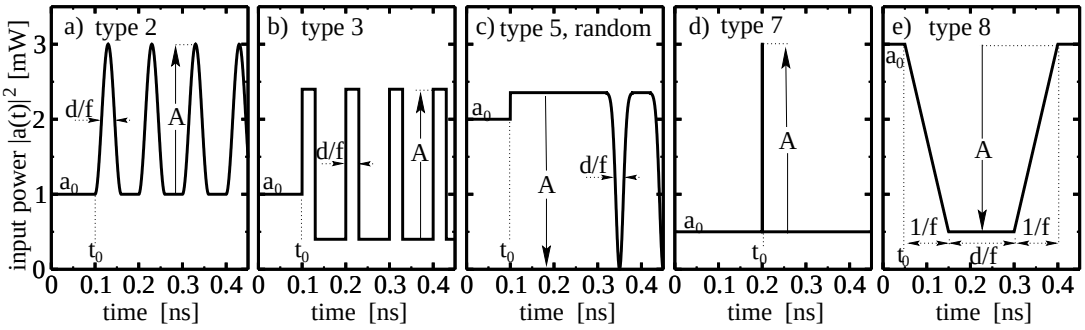

Figure 2: *Different profiles of the modulated optical injection power* $|a(t)|^2$.

It can be seen from the structure of a LDSL input data file given above that an optical injection can be applied also at junctions of the sections. This is not a physical injection, of course, but it can be useful when modeling multiple optical injections via the same facet. In this case one has to introduce a short fictive section S_0 with no gain, coupling or losses. One of the optical signals should be injected via the fictive facet at the left side of the section S_0, another signal should be injected via the junction of the sections S_0 and S_1, which corresponds to a realistic facet of the laser.

Let us discuss now the methods to investigate the quality of the self pulsating solutions occuring in the model described above.

3 Characteristics of the self pulsations

3.1 Analysis of the output in the frequency domain

Assume that we have computed a time series of the complex output field and its self pulsating power on the time interval $[0, T]$:

$$\psi^-(0, k\tau)|_{k=0}^M, \qquad \text{and} \qquad |\psi^-(0, k\tau)|^2|_{k=0}^M, \qquad M\tau = T \ \ (\text{s}). \tag{3}$$

We assume that f_0 (Hz) and $P_0 = 1/f_0$ (s) are the mean frequency and period of the self pulsating output power $|\psi^-(0, k\tau)|^2$ respectively. That is, the pulses in this sequence appear approximately with the period P_0 jittering around the mean value P_0, if they are not exactly periodic.

It is important to know the precise frequency of the SP in a free running laser, since it should be close to the frequency f_{ext} of external modulation. It was observed experimentally that a locking of the laser output to the external modulation can be realized when $|f_0 - f_{ext}|$ is not bigger then 150 - 200 MHz. Therefore, before applying an external modulated signal we need to have a good approximation (say, with ~ 10 MHz precision) of f_0.

A Fast Fourier Transform (FFT) applied to a discrete set of the data (3) allows to compute effectively the optical (see Fig. 1) and the power (see Fig. 3) spectrum of the signal. The main peak in the power spectrum shows immediately a frequency f_{FFT} (Hz) of the SP signal which, in general, is slightly different from the mean frequency f_0. Let us set $f_{FFT} = f_0 + \delta f$.

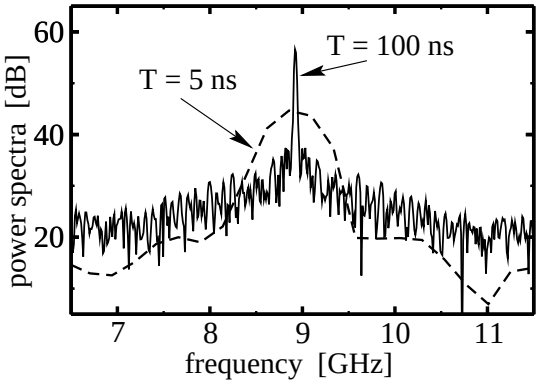

Figure 3: *Power spectrum of the same self pulsating output based on different time intervals* $[0, T]$. *Solid and dashed lines correspond to* $T = 100$ *(ns) and* $T = 5$ *(ns) respectively.*

It is well known that the minimal difference of two frequencies that can be estimated by means of the FFT is $1/T$ Hz. Therefore, the estimate $|\delta f| \leq 1/2T$ for the frequency error holds. This is one of the problems which arises when analysing a power spectrum of the output. Namely, in order to have a 10 MHz frequency resolution which implies 5 MHz bound for $|\delta f|$, one has to compute time series on a 100 ns interval, what requires a sufficiently large amount of computing time and memory. 5 ns intervals, which are in general sufficient to arrive at a stable stationary or SP state in the time domain, gives only a 200 MHz resolution in the

frequency domain (100 MHz bound for $|\delta f|$), which is not satisfactory for defining the frequency of SP or for measuring the width of the spikes in the power spectrum of the output (see Fig. 3).

It will be also shown later that even a small frequency error $\delta f \neq 0$ in the FFT can imply a poor representation of the possibly periodic signal when drawing "eye" diagrams (see Fig. 6(IIa)).

Summary of this subsection:

- *To have a satisfactory frequency resolution of the power spectrum one has to apply the FFT to computed data on sufficiently large time intervals, which requires large computing time and memory.*
- *Even for large T, f_{FFT} does not provide a precise mean frequency of SP.*
- *Even a small frequency error δf causes closed "eye" diagram when sampling at least $N = f_0/|\delta f|$ pulses computed on the $[0, 1/|\delta f|]$ time interval.*
- *In order to analyze the jitter of the pulses in the time domain, we need alternative algorithms to define the mean frequency of SP.*

In the sequel we will discuss the implemented tools to analyze the quality of SP in the time domain.

3.2 A definition of the mean frequency of SP

Let us return to the problem, how to determine properly the mean frequency f_0 and the corresponding period $P_0 = 1/f_0$ of a given self pulsating function $g(t) = |\psi^-(0,t)|^2$ defined on $[0,T]$. To fulfill this task correctly for the given function is quite difficult, especially if shapes of the consequent pulses of $g(t)$ are slightly different or if the applied noise implies jittering of the mean period.

Computations of the period P_0 and of the characteristics of the quality of SP are based on the series of the half height time moments $t_{i,k}$ and $t_{d,k}$, where increasing or decreasing part of the function $y = g(t)$ crosses the pulse half height line

$$y = M = [min(g(t)) + max(g(t))]/2.$$

In the case when noise or an optical injection are applied, an increasing (decreasing) part of each separate pulse can cross the line $y = M$ more than once. In this case, the half height moment $t_{i,k}$ (or $t_{d,k}$) will be defined as the mean value of the corresponding crossing points (see Fig. 4(a)).

The following algorithm allows to determine the mean frequency of SP:

- Find the minimal (A), the maximal (B) and the half height $M = (A + B)/2$ values of the $g(t)$.

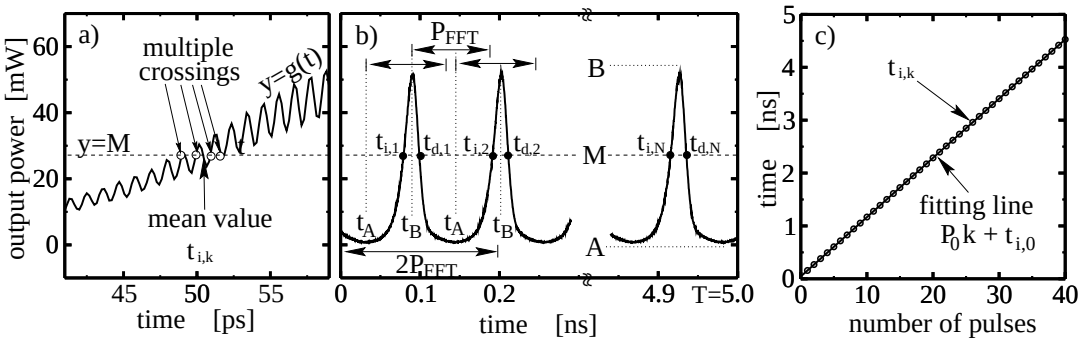

Figure 4: *a): Definition of the half height moment $t_{i,k}$ from several crossings of the positive slope of the pulse and line $y = M$. b): Pulse trace with identified time moments t_A and t_B corresponding to minima and maxima of $g(t)$ within each approximate period P_{FFT}. Solid points indicate the half height moments $t_{i,k}$ and $t_{d,k}$. c) Half height moments $t(k) = t_{i,k}$ are fitted with the line $t(k) = P_0 k + t_{i,0}$.*

- For SP with a good extinction ratio ($(A-B)/(A+B) > 0.2$) we continue our algorithm.
- Find the approximate frequency f_{FFT} and the corresponding period $P_{FFT} = 1/f_{FFT}$.
- Find the pulse minimum position t_A within the two first approximate periods (see Fig. 4(b)). Adjust an index $k = 1$.
- Starting from t_A, find the pulse maximum position t_B within one approximate period.
- Find the half height moment $t_{i,k}$ within the interval $[t_A, t_B]$.
- Starting from t_B, find the pulse minimum position t_A within one approximate period.
- Find the half height moment $t_{d,k}$ within the interval $[t_B, t_A]$.
- Repeat last four steps of the algorithm (see Fig. 4(b)) taking $k = k + 1$, until T is not reached.
- The half height moments $t(k) = t_{sl,k}|_{k=1}^{N}$ with $sl = i$ or $sl = d$ are approximating the line $t(k) = P_0 k + t_{sl,0}$ as in Fig. 4(c). The period P_0 and the frequency $f_0 = 1/P_0$ are found from the least square approximation.

Summary of this subsection:

- *The half height moments $t_{sl,k}$ describing mean intersection of the increasing ($sl = i$) or the decreasing ($sl = d$) slopes of the pulses with a half height line $y = M$ are defined.*

- *The algorithm defining the mean period and mean frequency of the given pulse sequence is given.*
- *If this sequence would be replaced by a shorter or a longer one, then the mean frequency and the period can slightly change, but in any case they are more precise than those evaluated from FFT.*

3.3 Different diagrams and jitter measures describing quality of SP

In order to analyze computed pulses and to determine their quality in the *time domain* the sampling technique (eye diagrams) can be used. For this reason, the computed signal $g(t) = |\psi^-(0,t)|^2$, $t \in [0,T]$ is sampled on the interval $[0,P]$ by means of the following mapping:

$$M : ([0,T]\times\mathbf{R}) \mapsto ([0,P]\times\mathbf{R}), \qquad M([t,g(t)]) = \Big[P\Big\{\frac{t}{P}\Big\}, g(t)\Big],$$
$$\Big\{\frac{t}{P}\Big\} = \frac{t}{P} - k \in [0,1), \qquad k \in \mathbf{N}.$$

As a rule, when investigating periodic or quasi-periodic SP of a free running laser, or of a laser with constant power optical injection, the sampling interval length P should be adjusted to the already computed (see previous subsection) mean period $P_0 = 1/f_0$.

Let us introduce the notion of the *relative phase* (RP) $\phi_{sl}(k,P)$ with $sl = i$ or $sl = d$:

$$\phi_{sl}(k,P) = (t_{sl}(k) - Pk)/P. \tag{4}$$

This value will characterize the relative phase between the corresponding half height moments and some P-periodic function.

Whenever P is equal to the mean period P_0 of the pulse sequence, these relative phases should deviate from some constant value for the different pulses (see, e.g., Fig. 5(Ib,IIb,IIIb)). Otherwise, if $P \neq P_0$, the RP $\phi_{sl}(k,P)$ will deviate from some slant line (see Fig. 6(Ib,IIb)).

After sampling such SP with period $P = P_0$, we represent and characterize the SP by the following diagrams:

- The "eye" diagrams as depicted in Fig. 5(Ia-IIIa).
- The "TRP" diagrams represented in Fig. 5(Ib-IIIb) show the traces of the relative phases $\phi_{sl}(k,P)$ defined in (4) of the pulses with respect to a P-periodic function. These "TRP" diagrams represent a similar situation as Fig. 4(c), where the half height moments $t_{sl,k}|_{k=1}^{N}$ are distributed around the approximating line $t_{sl} = P_0 k + t_{sl,0}$. As units of the ordinate axis in the "TRP" diagram we can choose parts of the sampling period P or picoseconds (drawing $\tilde{\phi}_{sl}(k,P) = P \cdot \phi_{sl}(k,P)$ instead of $\phi_{sl}(k,P)$) as well.

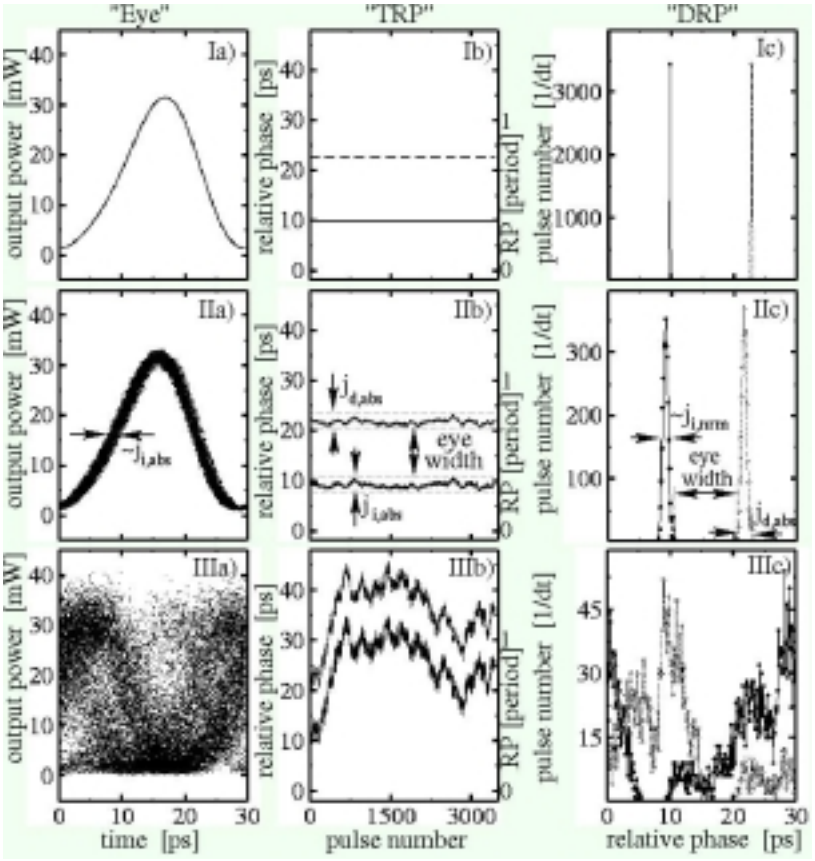

Figure 5: *(a) "Eye", (b) "TRP", (c) "DRP" diagrams. I): Ideal periodic case without noise. II): Realistic value of noise. III): 30 times larger level of noise than in the case II.*

- The "DRP" diagrams in Fig. 5(Ic-IIIc) represent the distribution of the relative phases $\phi_{sl}(k,P)$ (or $\tilde{\phi}_{sl}(k,P)$) within the sampling period.

To characterize the jitter of pulses, we use two different measures:

- The *absolute* jitter of the increasing ($j_{i,abs}$) or the decreasing ($j_{d,abs}$) slope of a pulse is defined by

$$j_{sl,abs} = \max_k\{\phi_{sl}(k,P)\} - \min_k\{\phi_{sl}(k,P)\}, \qquad sl = i,d,$$

  and is shown in Fig. 5(IIbc).

- Assume, that the locations of the relative phases $\phi_{sl}(k,P)$, $sl = i,d$ are described by the Gaussian distribution with mean value ξ_{sl} and dispersion σ_{sl}. The *normal* jitter $j_{i,nrm}$ (or $j_{d,nrm}$) is defined by the full width at half maximum of this distribution

$$j_{sl,nrm} = 2\sigma_{sl}\sqrt{\ln 4}, \quad \sigma_{sl} = \sqrt{\sum_{k=1}^{N} \frac{(\phi_{sl}(k,P) - \xi_{sl})^2}{N-1}}, \; \xi_{sl} = \sum_{k=1}^{N} \frac{\phi_{sl}(k,P)}{N} = t_{sl,0},$$

  and is depicted in Fig. 5(IIc).

Fig. 5 represents SP at ~ 33 GHz of a model of a 3 section DFB laser with two active DFB sections whose stop-bands do not overlap. The SP depicted in I,II and III differ only by the applied level of noise:

- Fig. 5(I): no noise, the signal $|\psi^-(0,t)|^2$ is periodic with the exact period $P = P_0 = 1/f_0$. The different sampled pulses precisely overlap and could not be distinguished (Fig. 5(Ia)). There is no drift of the RP $\phi_{sl}(k, P_0)$ from the horizontal lines $t = t_{sl,0}$ and both measures of the jitter are almost zero (Fig. 5(Ibc)).
- Fig. 5(II): a "realistic" level of noises is applied. The SP are no more exactly periodic. Nevertheless, an open "eye" in Fig. 5(IIa) is clearly seen. Different pulses do not overlap each other precisely, but their random drift around some mean position is not very large. Such a drift of the RP together with the jitter measures is shown in Fig. 5(IIbc).
- A much higher level of the noise causes a closing of the "eye" in Fig. 5(IIIa). The figures 5(IIIbc) are still representing the random nature of the pulse drift around some mean value. A distribution of the RP shown in Fig. 5(IIIc) can be still considered as Gaussian, if we will shift a part of the indicated data by one sampling period.

Summary of this subsection:

- *The notion of the* relative phase *(RP) between pulses of the SP and P-periodic function is introduced in (4).*
- *Three types ("eye", "TRP", "DRP") of diagrams based on a sampling of the SP and on a location of the RP are presented.*
- *An absolute and a normal measures for a jitter are introduced.*
- *The "TRP" and the "DRP" diagrams yield information about the absolute and the normal jitter respectively.*
- *The dependence of the quality of SP on the level of noise is presented.*

3.4 Influence of a small error in defining the sampling period

Let us assume that the sampling frequency f (and the period $P = 1/f$) differs from the mean frequency f_0 (and the period $P_0 = 1/f_0$) with the frequency error $\delta f = f_0 - f \neq 0$. This error implies an error of the number of periods in the time interval $[0, T]$. Now really computed (non-integer number) $N_0 = Tf_0$ pulses are incorrectly treated and sampled as (non-integer number) $Tf = N_0 + T\delta f \neq N_0$ pulses.

In these cases one should be quite careful when interpreting diagrams and jitter of the SP:

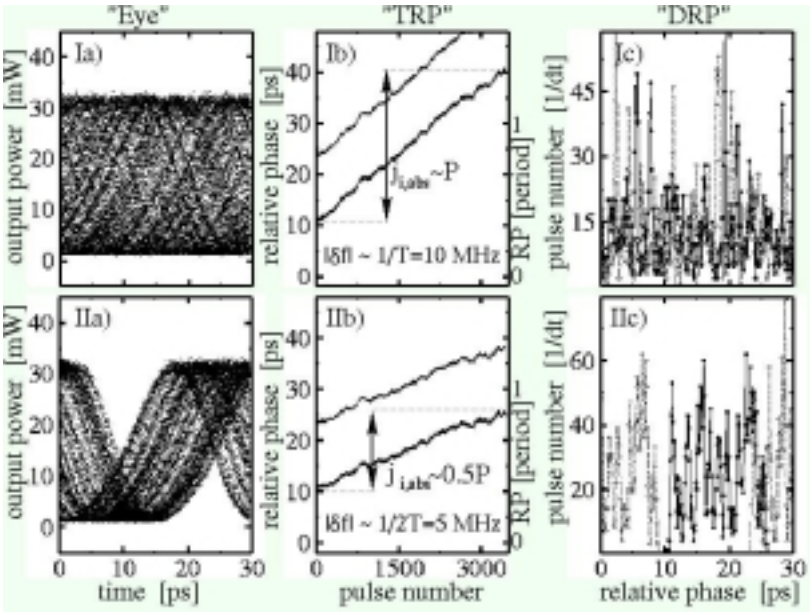

Figure 6: *The diagrams represent the same SP as in Fig. 5(II) with an error of sampling frequencies and periods. I): The frequency error $1/T$ causes a total closing of the "eye". II): The frequency error $1/2T$ implies a half period drift of the pulses (their RP) and almost closed "eye".*

- When sampling the given pulses with an incorrect period $P = 1/f$, an artificial drift of the probably good signal (its RP) in the "eye" diagram will be observed (see Fig. 6(Ia,IIa)).
- Such a drift of the RP $\phi_{sl}(k, P)$ will be approximately equal to $T\delta f \cdot P$ seconds or $T\delta f$ sampling periods and will be wrongly interpreted as a jitter of SP (see Fig. 6(Ib,IIb)).
- In case $|T\delta f| = 1/2$, which can arise in estimating the sampling frequency f by the FFT ($f = f_{FFT}$), the drift of the pulses (their RP) is equal to $P_{FFT}/2$ and, therefore, the "eye" in the corresponding diagram in Fig. 6(IIa) will be almost closed.

To avoid such misleading interpretation of the diagrams above and of the size of the jitter one has to look more carefully at the "TRP" and the "DRP" diagrams in Fig. 6(Ibc,IIbc):

- It seems that the assumption of a Gaussian distribution of the RP in the "DRP" diagrams in Fig. 6(Ic,IIc) is not correct.
- A better indication of the error in defining the sampling period can be provided by the "TRP" diagrams in Fig. 6(Ib,IIb). Here the RP $\phi_{sl}(k, P)$ are drifting not around the *horizontal* line $t = t_{sl,0}$, but around some slant line $t = Ck + t_{sl,0}$, where $C \approx P_0 - P \approx -\delta f / f^2$ is determined by the frequency error δf.

Summary of this subsection:

- *The frequency error which arises in defining the sampling frequency can cause an overestimation of the jitter and a closing of the "eye" diagrams.*

- *This frequency error can be recognized from the "TRP" diagrams, if the RP are drifting around some slant line.*

3.5 Closing of the "eye" diagram due to an optical injection

The superposition of an optical injection with the optical field of the laser leads to high frequency oscillations along the "slowly" pulsating output power. An example of such fast oscillations for an increasing slope of the single pulse is given in Fig. 4(a). If the optical signal is strong enough, then these oscillations are visible in the computed signal and can even cause a closing of the "eye" diagram.

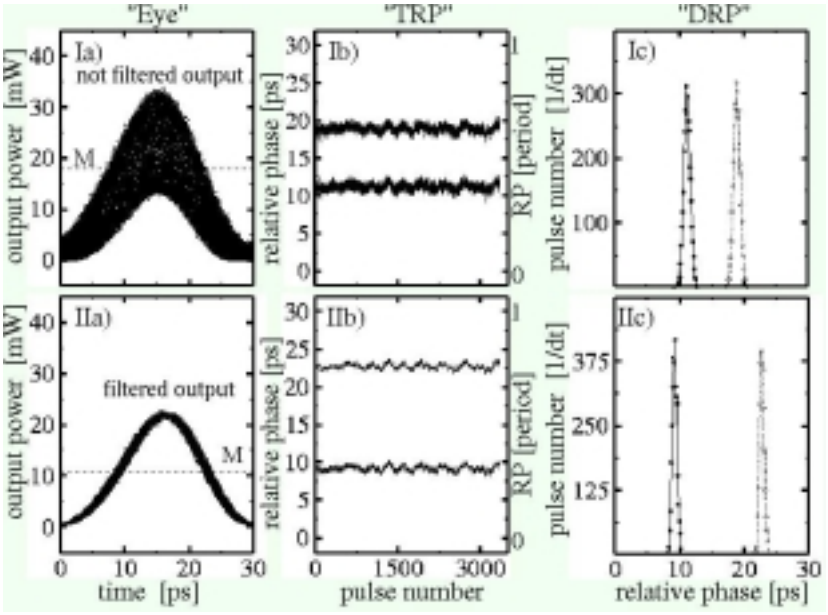

Figure 7: *The diagrams representing the same SP as in Fig. 5(II) with an applied 4 mW constant power optical injection at −8 nm relative wavelength. I): Output signal without filtering. II): Filtered output signal.*

The discussion of these diagrams suggests how to recognize this situation and to avoid a wrong interpretation of the bad quality of the SP:

- The fast oscillations due to superposition of signals at different wavelengths cause a broadening of each separate pulse as in Fig. 4(a) as well as a broadening of the sampled pulses in the eye diagram in Fig. 7(Ia).
- To define the half height moments we have to take into account only mean values of the multiple crossings of each pulse with the mean line $y = M$ (see white points in Fig. 4(a)).
- The drift of the pulses visible in the "eye' diagram 7(Ia) is much higher than the introduced measures of the jitter (see 7(Ibc)), which take into account only drift of the relative phases.
- In order to suppress an influence of the optical injection we filter the output field $\psi^-(0,t)$ with a Lorentzian filter, given by the following relation between

the complex amplitudes of the input $A_{inp}(\omega)$ and of the output $B_{out}(\omega)$ in the optical frequency domain:

$$B_{out}(\omega) = \Big(\frac{|\omega_{inject} - \omega_{lasing}|}{|\omega_{inject} - \omega_{lasing}| + i(\omega - \omega_{lasing})}\Big)^{10} A_{inp}(\omega).$$

This filter exhibits approximately a 15 dB amplitude suppression at wavelengths of the injection and only a small suppression for the lasing wavelengths. The resulting filtered output is represented in Fig. 7(II), and do not differs significantly from the original signal in the laser without the injection shown in Fig. 5(II).

Summary of this subsection:

- *The superposition of an injected relatively strong optical signal with the optical field induced by the laser can close the "eye" diagram.*
- *The jitter measures $j_{abs,nrm}$ can be much smaller than the jitter at a half height of the pulses visible in the "eye" diagrams.*
- *The jitter induced by an optical injection can be removed from the "eye" diagrams by filtering the output signal.*

4 Applications

4.1 Locking of SP

If we investigate locking of self pulsations, then the sampling period P is determined by the period of the external modulated signal $P_{ext} = 1/f_{ext}$. It is known that in order to achieve locking, the modulation frequency f_{ext} should be close to the mean frequency f_0 of the free running laser.

Let us again consider a 3 section laser with 2 active DFB sections demonstrating SP at $f_0 \approx 33$ GHz (see Fig. 5(II)). To have a more precise representation of the same signal, we computed it on a $T = 400$ ns time interval. Assume that the electrical modulation with the amplitude A and the frequency $f_{ext} = f_0 + \delta f$, $\delta f = 50$ MHz is applied to one of the DFB sections.

The transition from the unlocked to the locked state is shown in the Fig. 8 and will be discussed below:

- For reference, in Fig. 8(I) shows the SP of the laser without modulation ($A = 0$) sampled with its mean period P_0.
- Next we consider a sampling of the signal with the modulation period $P = P_{ext}$. For a small modulation amplitude $A \approx 0$ the locking can not be realized. The

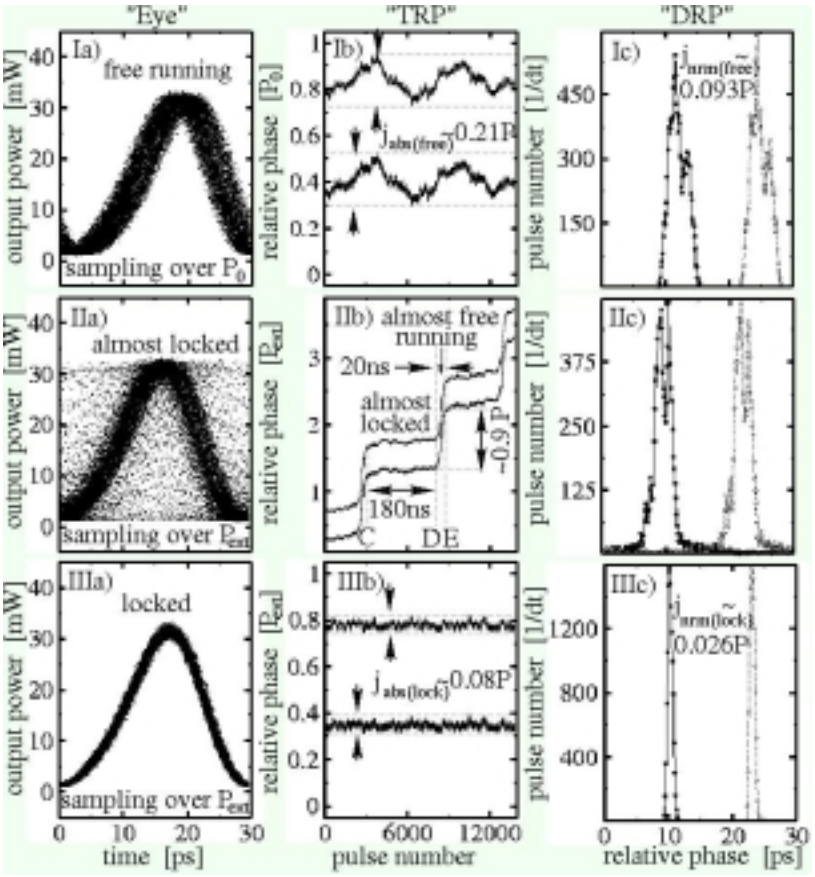

Figure 8: *The diagrams represent the transition from the SP at $f_0 \approx 33$ GHz in the free running laser towards the locked SP at $f_{ext} = f_0 + 50$ MHz. I): SP of the free running laser ($A = 0$) sampled with its mean period P_0. II): Unlocked situation at $A = 3.35$ mA. Sampling was made with $P = P_{ext}$, the amplitude A is close to its critical value where locking can be detected. III): The locked SP with $A = 6$ mA.*

sampling period P_{ext} is different from the mean period P_0 and, therefore, the "eye" diagram will be closed as in Fig. 6(Ia), if a sufficiently large number of the pulses will be applied. Otherwise the situation in Fig. 6(IIa) should be observed. The computed output over $T = 400$ ns guarantees that the drifting relative phases $\phi_{sl}(k, P_{ext})$ along a slant line in the "TRP" diagram will cover $T \cdot \delta f = 20$ periods, i.e., $j_{sl,abs} \approx 20$ (periods).

- At some amplitude ($A \approx 3.45$ mA in our case), still being unlocked, the laser strongly "feels" a modulation of the signal. The "eye" is still closed (see Fig. 8(IIa)), but a "stairway" form of the "TRP" diagram indicates intervals, where the SP is almost locked, (an interval $[C, D]$ in Fig. 8(IIb)).

- On the interval $[C, D]$ (Fig. 8(IIb)) the relative phases $\phi_{sl}(k, P_{ext})$ are drifting along almost horizontal lines, indicating a coincidence of the frequencies of SP and external signal.

- Afterwards, during the much shorter interval $[D, E]$, an almost linear increase of the RP indicates that the difference between the SP and external frequencies is approximately equal to

$$\delta\tilde{f} \approx N_{periods}/T_{int} = 0.9 \text{ (periods)} \ /20 \text{ (ns)} = 45 \text{ MHz}.$$

This value is close to the $\delta f = 50$ MHz, which is a difference between the frequency f_0 of the free running SP and the modulation frequency f_{ext}.

- Approximately at the position D the locking is lost and during the interval $[D, E]$ the self pulsations are running with their own (free running) frequency f_0. The RP is changing during $[D, E]$ by almost one period and approximately at the position E it reaches similar "locking" conditions (with a shift of one period) as at the position C. Here a new "locking" interval starts, where the RP exhibits only a drift around the horizontal line.

- In such regimes one needs to apply long enough data sequence: if, by chance, only a sequence of the data from the interval $[C, D]$ (corresponding to a quite long 180 ns time interval) would be considered, an open "eye" diagram would be seen. The study of the "TRP" diagram within the interval $[C, D]$ in Fig. 8(IIb) in general will also indicate the already achieved locking. Due to this problem, it is a very time consuming task to detect an exact value of the amplitude A, where the locking starts to be realised.

- Finally, at the sufficiently big amplitude ($A = 6$ mA in our case) the laser is locked to the frequency f_{ext}, a nice open "eye" is visible in Fig. 8(IIIa), a jitter of the locked solution is clearly smaller than a jitter of the SP in the free running laser (see 8(IIIbc)).

Summary of this subsection:

- *The diagrams allow us to analyze a transition of the SP from the unlocked state ($A \approx 0$) to the locked state.*

- *A detection of the exact amplitude A where locking is achieved for the first time requires very time consuming computations. It can be difficult to distinguish locked and unlocked regimes close to this precise value of A.*

- *At least in the demonstrated case, locked SP performs a smaller jitter than SP in the free running laser.*

4.2 The quality of SP for different phases φ

Let us introduce the phase parameter $\varphi = 2l_{phas}\delta_{phas}/2\pi$ which is related to the detuning δ (see (1)) in the passive phase tuning section.

It is known that tuning of the phase conditions φ in the phase section implies a transition from the stationary lasing states to self pulsations, or a transition to different regions of self pulsations (see [1, 5]).

In our previous examples we demonstrated ~ 33 GHz self pulsations which were observed for the phase $\varphi = 0.8$ which is located in a middle of the phase interval $[0.66, 0.92]$ with frequency $f_0 \in [31, 39]$ GHz.

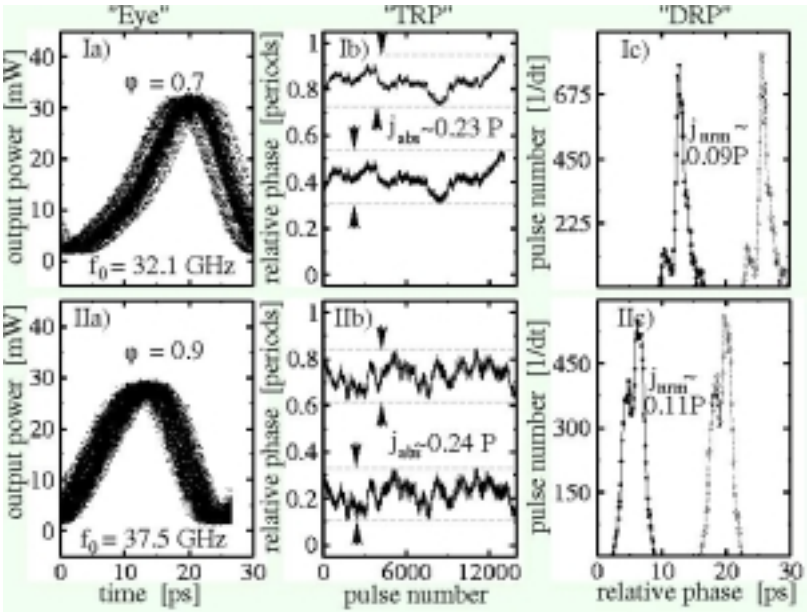

Figure 9: *Quality of SP in the free running laser for the phases $\varphi = 0.7$ (I) and $\varphi = 0.9$ (II).*

The following figure and the discussion are concerned with self pulsations close to the border of this interval:

- For the phases $\varphi = 0.7$ and $\varphi = 0.9$ the jitter of SP in the free running laser is similar to the jitter of SP for the reference phase $\varphi = 0.8$ indicated in Fig. 8(I).
- The frequencies of SP can be continuously tuned from ~ 31 GHz up to ~ 39 GHz by tuning the phase parameter φ.

The ability of these SP to synchronize with a modulated current injection was also checked:

- The modulation frequency $f_{ext} = f_0 + 50$ MHz as in Fig. 8, or $f_{ext} = f_0 - 50$ MHz was considered.
- It was observed that for a fixed phase φ the required modulation amplitude in any of the DFB sections (A_1 or A_3) is approximately the same for both frequency offsets ($\delta f = \pm 50$ MHz).
- Surprisingly, the "critical" value of the amplitudes A_1 and A_3 are similar and are sensitively dependent for different phases. It has been found that $A_1|_{\varphi=0.7} \approx 4.5$ mA, $A_1|_{\varphi=0.8} \approx 3.4$ mA (see Fig. 8(II)), and $A_1|_{\varphi=0.9} \approx 2.2$ mA.
- The locking ranges for the different phases when modulating injection in the both DFB sections or when applying an optical modulated signal will be discussed in more details in the following report.

Summary of this subsection:

- *The frequency of SP in the free running laser can be tuned in certain range by tuning the phase parameter φ.*
- *It seems that the quality of SP in the free running laser for different values of φ is quite similar.*
- *The locking ranges are quite different for SP for different phases φ.*

4.3 The influence of the internal reflectivities

It is supposed that the optical fields $\psi^{\pm}$ can be reflected from junctions between different sections:

$$\psi^{+}_{out} = r_{junct}\,\psi^{-}_{inc} + \sqrt{1-|r_{junct}|^2}\,\psi^{+}_{inc}, \qquad \psi^{-}_{out} = -r^{*}_{junct}\,\psi^{+}_{inc} + \sqrt{1-|r_{junct}|^2}\,\psi^{-}_{inc}.$$

Here, the complex parameter r_{junct}, $|r_{junct}| \leq 1$ should be adjusted to each of the laser section junctions.

The influence of the internal reflectivities to the quality of SP is as follows:

- In the ideal case we have adjusted $r_{junct} = 0$ at each junction. It is clear that while this parameter remains small enough, it should not have a big influence onto the SP observed in the laser.
- When the reflectivity amplitude $|r_{junct}|$ grows, then a transition of the initial $30-40$ GHz frequency SP to another region of SP with different frequencies or to the some other solution can be observed. These transitions will be observed later, if our parameters (e.g., phase φ) of an "ideal" ($r_{junct} = 0$) laser are located in the middle of the parameter region with similar SP.
- Such a situation is represented in Fig. 10, where SP with $|r_{junct;1,2}| = 0.075$ for $\varphi = 0.8 \in [0.66, 0.92]$ are indicated. Similar SP in the "ideal" laser have been considered earlier (e.g., in Fig. 8).
- The phases of the complex reflectivity coefficients $r_{junct;1,2}$ also play an important role. When selecting these phases arbitrary, one can find quite good SP with good locking properties. Such SP in general can be of the same or even better quality as SP with $r_{junct;1,2} = 0$ (see, e.g., Fig. 10(I,II) and compare with Fig. 8(I,III)).
- Nevertheless, when taking other phases of the coefficients r_{junct}, the quality as well as the locking of SP can become much worse (see Fig. 10(III,IV)).
- One can improve the SP indicated in Fig. 10(III,IV) by slightly tuning the parameter φ. Nevertheless, we have tested that such SP become worse again by readjusting phases of r_{junct}.

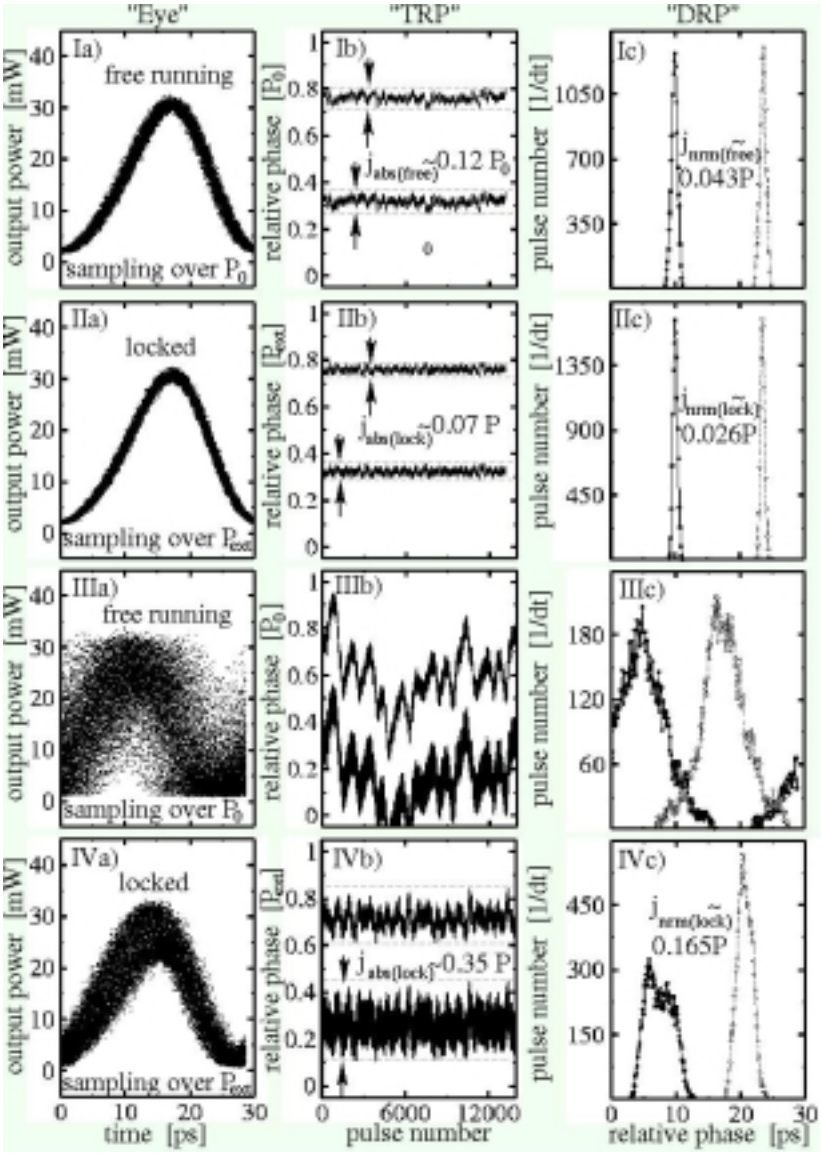

Figure 10: *SP for $\varphi = 0.8$ when internal reflectivities are applied. I,II): $r_{junct,1} = 0.075 \cdot e^{i2\pi \cdot 0.7}$ and $r_{junct,2} = 0.075 \cdot e^{i2\pi \cdot 0.3}$. III,IV): $r_{junct,1} = r_{junct,2} = 0.075$. the diagrams I and III indicate SP in the free running laser, while diagrams II and IV show locking at the modulation frequency $f_{ext} = f_0 + 50$ MHz and with the amplitude $A_1 = 6$ mA. First the locking of SP was observed for $A_1 = 4.9$ mA (I,II diagrams), and for $A_1 = 3.6$ mA (III,IV diagrams). Note a bad performance of SP in III,IV diagrams.*

- When using larger amplitudes $|r_{junct}|$ (say, $|r_{junct}| = 0.1$), even a shift of φ does not help to return to a required region of SP at $30 - 40$ GHz frequency.

Summary of this subsection:

- *The internal field reflectivities at the junctions of the sections can cause different dynamical behaviour of the laser than predicted by the "ideal" model without such reflectivities.*
- *The importance of both the amplitude and the phase of such reflectivities was has been demonstrated.*

5 Conclusions

Possibilities of LDSL tool to investigate and to characterize the quality of SP and their locking behaviour were discussed. Useful characteristics, such as temporal drift and distribution of the relative phases were introduced and discussed. Advantages of these characteristics with respect to the conventional "eye" diagrams have been demonstrated. An influence of some selected parameters such as phase condition, noise or internal reflectivity on the quality of SP have been also discussed.

References

[1] U. Bandelow, H.-J. Wünsche, B. Sartorius, M. Möhrle, "Dispersive self-Q-switching in DFB lasers: Theory versus experiment", *IEEE J. Selected Topics in Quantum Electron.* **3**, pp. 270-278, 1997.

[2] M. Radziunas, H.-J. Wünsche, B. Sartorius, O. Brox, D. Hoffmann, K. Schneider, D. Marcenac "Modeling Self-pulsating DFB Lasers with an Integrated Phase Tuning Section", *IEEE J. Quantum Electron.* **36**, pp. 1026–1034, 2000.

[3] M. Radziunas, H.-J. Wünsche, "Dynamics of multi-section DFB semiconductor laser: traveling wave and mode approximation models", *WIAS-Preprint* **713**, 2002.

[4] A.A. Tager, K. Petermann, "High-frequency oscillations and self-mode locking in short external-cavity diodes", *IEEE J. Quantum Electron.* **30**, pp. 1553, 1994.

[5] M. Möhrle, B. Sartorius, C. Bornholdt, S. Bauer, O. Brox, A. Sigmund, R. Steingrüber, M. Radziunas, H.-J. Wünsche, "Detuned grating multi-section-RW-DFB-lasers for high speed optical signal processing", *IEEE J. Selected Topics in Quantum Electron.* **7**, pp. 217-223, 2001.

[6] U. Bandelow, M. Radziunas, J. Sieber, M. Wolfrum, "Impact of Gain Dispersion on the Spatio-temporal Dynamics of Multisection Lasers", *IEEE J. Quantum Electron.* **Vol. 37 2**, pp. 183-189, 2001.

[7] H.-J. Wünsche, O. Brox, M. Radziunas, F. Henneberger, "Excitability of a semiconductor laser by a two-mode homoclinic bifurcation", *Phys. Rev. Lett.* **88(2)**, pp. 23901, 2002.

[8] M. Radziunas, "Documentation of Longitudinal Dynamics in Semiconductor Lasers (LDSL) tool", *to appear in WIAS – Technical Report series*, 2002.